Precision neutron interferometric measurement of the n-^{3}He coherent neutron scattering length

P. R. Huffman,[1,2] D. L. Jacobson,[2] K. Schoen,[3] M. Arif,[2] T. C. Black,[4] W. M. Snow,[5] and S. A. Werner[3,2]
[1]*North Carolina State University, Raleigh, North Carolina 27695, USA*
[2]*National Institute of Standards and Technology, Gaithersburg, Maryland 20899-8461, USA*
[3]*University of Missouri-Columbia, Columbia, Missouri 65211, USA*
[4]*University of North Carolina at Wilmington, Wilmington, North Carolina 28403-3297, USA*
[5]*Indiana University/IUCF, Bloomington, Indiana 47408, USA*
(Received 10 March 2004; published 15 July 2004)

A measurement of the n-^{3}He coherent scattering length using neutron interferometry is reported. The result, $b_c=(5.8572\pm0.0072)$ fm, improves the measured precision of any single measurement of b_c by a factor of eight; the previous world average, $b_c=(5.74\pm0.04)$ fm, now becomes $b_c=(5.853\pm0.007)$ fm. Measurements of the n-p, n-d, and n-^{3}He coherent scattering lengths have now been performed using the same technique, thus allowing one to extract the scattering length ratios: parameters that minimize systematic errors. We obtain values of $b_{n^3\mathrm{He}}/b_{np}=(-1.5668\pm0.0021)$ and $b_{nd}/b_{np}=(-1.7828\pm0.0014)$. Using the new world average value of b_c and recent high-precision spin-dependent scattering length data also determined by neutron optical techniques, we extract new values for the bound singlet and triple scattering lengths of $b_0=(9.949\pm0.027)$ fm and $b_1=(4.488\pm0.017)$ fm for the n-^{3}He system. The free nuclear singlet and triplet scattering lengths are $a_0=(7.456\pm0.020)$ fm and $a_1=(3.363\pm0.013)$ fm. The coherent scattering cross section is $\sigma_c=(4.305\pm0.007)$ b and the total scattering cross section is $\sigma_s=(5.837\pm0.014)$ b. Comparisons of a_0 and a_1 to the only existing high-precision theoretical predictions for the n-^{3}He system, calculated using a resonating group technique with nucleon-nucleon potentials incorporating three-nucleon forces, have been performed. Neutron scattering length measurements in few-body systems are now sensitive enough to probe small effects not yet adequately treated in present theoretical models.

DOI: 10.1103/PhysRevC.70.014004 PACS number(s): 03.75.Dg, 07.60.Ly, 61.12.−q

I. INTRODUCTION

Over the last few years a combination of computational and theoretical advances has led to a qualitative improvement in calculations of the properties of few-nucleon systems starting from the extensive data on the nucleon-nucleon (NN) interaction [1–9]. The most precise data available to compare to these new calculations are few-nucleon binding energies and energy levels, which in most cases are extremely well known. These calculations should also be able to accurately predict the low-energy scattering observables such as the S-wave scattering lengths in the various few-nucleon systems.

Neutron interferometric methods for measuring the coherent scattering length, which is the linear combination of scattering lengths that gives rise to the optical potential of a neutron in a medium, have now reached precisions better than 10^{-4} in certain nuclei [10]. This precision is now high enough to severely test the models if the measurements are conducted in few-body systems. We have recently reported a very precise measurement of the bound coherent n-d scattering length [11,12]. New calculations of the n-d scattering lengths utilizing modern NN potentials have also recently been reported [13]. These measurements, combined with the new calculations, reveal that all modern NN potential models, with and without three-nucleon forces, and with and without electromagnetic interactions, fail to reproduce the experimental bound coherent n-d scattering length.

In this article, we report a measurement of the bound coherent scattering length in the n-^{3}He system. In this particular case, there is a recent high-precision measurement [14] of the incoherent scattering length using the technique introduced by Abragam *et al.* [15] of nuclear pseudomagnetic precession of polarized neutrons in a polarized target. We are therefore able to extract new high-precision values of the separate scattering lengths in both S-wave channels of the n-^{3}He system. Again, a comparison with the most accurate available calculation for this system shows significant differences between theory and experiment. Taken together, these results suggest that neutron scattering length measurements are now sensitive to effects in nuclear few-body systems such as three-nucleon forces and charge symmetry breaking—effects that are still poorly understood.

Yet another motivation for increased precision in neutron scattering length measurements stems from the recent development of effective field theories (EFT) for low-energy nuclear systems. EFTs have engendered renewed optimism and excitement that a description of nuclear forces and few-nucleon systems may soon be achieved that is both conceptually and quantitatively accurate. Effective field theories separate nuclear interactions into two energy regimes; those above and those below some physically meaningful energy threshold, i.e., the pion mass. Below threshold, all possible diagrams consistent with the symmetries of the system are explicitly calculated in a perturbative scheme in which higher-order terms are suppressed by factors of the ratios of low excitation energies to the higher scale. Contributions from higher-energy processes are parametrized by a short-range, mean-field potential whose strength in a given channel is fixed by experimentally determined low-energy constants that are sensitive to the channel in question. As each new order of low-energy diagrams is considered, increased descriptive power is obtained and new interaction mechanisms appear. Each additional order requires another low-energy observable to constrain the mean-field behavior. The principal virtue of the EFT approach is the theoretical coherence it imposes on the study of low-energy systems. The complete physics appropriate to any order of calculation is inherent to the method, at least as rigorously implemented. In principle, model dependence is reduced to the choice of the threshold and the number of orders calculated.

Tactically, the EFT paradigm implies a new interdependence and interactivity between theory and experiment, both in constructing the calculation and in analyzing the result. Because each order of calculation requires as input the accurate determination of an additional low-energy parameter, the success of this technique relies critically on high precision measurements of low-energy observables such as binding and excitation energies and scattering lengths. In the case of the *n-d* system, for example, a scattering length is known to fix the lowest-order constant in an EFT approach [16]. From an EFT point of view, we expect that our measurement in the n-^{3}He system will provide the same essential input to future EFT calculations of the four-nucleon system that the *n-d* measurement already provides for the three-nucleon ($3N$) system.

II. NEUTRON OPTICS THEORY

The neutron and the ^{3}He nucleus are both spin $1/2$ objects that form total spin singlet ($S=0$) and spin triplet ($S=1$) scattering states. The coherent scattering length is proportional to the part of the scattering amplitude of the system that leaves the quantum mechanical state of the target unchanged and is therefore connected to the optical potential of the neutron in the medium. For *S*-wave scattering appropriate at the very low (few-meV) neutron energies used in our measurement, the relation between the nuclear coherent scattering length a_c and the scattering lengths in the singlet and triplet channels, a_0 and a_1, respectively, is given by

$$a_c = \tfrac{1}{4}a_0 + \tfrac{3}{4}a_1. \tag{1}$$

The bound coherent scattering length, b_c, is related to the free nuclear scattering length, a_c, by

$$b_c = \frac{m_n + m_{^3\mathrm{He}}}{m_{^3\mathrm{He}}} a_c, \tag{2}$$

where m_n is the neutron mass and $m_{^3\mathrm{He}}$ is the mass of the ^{3}He atom.

The bound coherent scattering length is one particular linear combination of the triplet and singlet scattering lengths. Knowledge of some other combination, in particular the bound incoherent scattering length b_i, given by

$$b_i = \frac{\sqrt{3}}{4}(b_1 - b_0), \tag{3}$$

allows one to independently extract the singlet and triplet bound scattering lengths b_0 and b_1, and hence the free nuclear scattering lengths a_0 and a_1.

The phase shift measured in neutron interferometry is proportional to the real part of the *S*-wave coherent scattering amplitude in the medium. It is important to be precise about the definition of this scattering amplitude in our case because the large absorption cross section for ^{3}He gives rise to an imaginary part to the scattering amplitude that cannot be neglected in the expression for the phase shift. Here we briefly review the origin of this relation [17].

In nonrelativistic potential scattering, the wave function at large distances from the scattering center takes the form

$$\psi = e^{i\vec{k}\cdot\vec{r}} + \frac{e^{ikr}}{r} f(\theta), \tag{4}$$

where $\vec{k}$ is the incident wave vector and $f(\theta)$ is the scattering amplitude. Let $\eta = \eta_r + i\eta_i$ be the (complex) *S*-wave phase shift in the partial wave expansion for the scattering amplitude. In terms of the *S*-wave phase shift, one can express the scattering amplitude and the scattering, absorption, and total cross sections as

$$f(\theta) = \frac{1}{2ik}(e^{2i\eta} - 1), \tag{5}$$

$$\sigma_s = \frac{2\pi}{k^2} e^{-2\eta_i}[\cosh 2\eta_i - \cos 2\eta_r], \tag{6}$$

$$\sigma_a = \frac{2\pi}{k^2} e^{-2\eta_i} \sinh 2\eta_i, \tag{7}$$

$$\sigma_t = \sigma_a + \sigma_s = \frac{2\pi}{k^2}(1 - \cos 2\eta_r e^{-2\eta_i}). \tag{8}$$

As can be seen, the expression for σ_t obeys the optical theorem. Since $2\pi/k^2 = 1.2\times 10^8$b for the neutron wavelength of $\lambda = 0.27$ nm used in this work, and $\sigma_a = 1\times 10^4$b, the *S*-wave phase shift $2\eta \approx 1\times 10^{-4} \ll 1$. Therefore, the wave function for *S*-wave scattering takes the form

$$\psi = \frac{\eta}{kr} + 1 + \cdots = \frac{\alpha_{-1}}{r} + \alpha_0 + \cdots \tag{9}$$

in the $r\to 0$ limit to 1×10^{-4} accuracy.

Now when one solves the Schrodinger equation in a solid by assuming a solution of the form

$$\psi = \chi(\vec{r}) e^{i\vec{k}'\cdot\vec{r}} \tag{10}$$

for the coherent wave in the medium, the small range of the neutron-nucleus potential relative to the atomic spacings means that the source term in the inhomogeneous differential equation is dominated by the $r\to 0$ singularity of the spherical waves emitted from all the scattering centers in the solid:

$$(\nabla^2 + k^2)\psi(\vec{r}) = -4\pi\alpha_{-1}\sum_n e^{i\vec{k}'\cdot\vec{r}}\delta(\vec{r} - \vec{r}_n). \tag{11}$$

Upon expanding $\chi(\vec{r})$ in a Fourier series and concentrating on solutions appropriate to a uniform medium for which the in-medium wave vector k' is close to the incident wave vector k, one gets the following relation between the dominant term in the Fourier expansion, proportional to α_{-1}, and the plane-wave term α_0:

$$\frac{\alpha_0}{\alpha_{-1}} = \frac{4\pi N}{(k'^2 - k^2)}, \tag{12}$$

where N is the number density in the medium. This ratio for an incident plane wave of unit amplitude $\alpha_0 = 1$ is the (complex) coherent scattering amplitude b_c.[1] Using the definition of the index of refraction $k' = nk$, also complex in general, we obtain the (complex) phase shift

$$\phi = k(1-n)D = -\lambda N D b_c, \tag{13}$$

where D is the thickness of the sample. Alternatively, one can express the phase shift in terms of a (complex) index of refraction as follows:

$$n^2 - 1 = \frac{N}{k^2}[\sqrt{4\pi\sigma_s - k^2\sigma_a^2} + ik\sigma_a]. \tag{14}$$

Therefore, the real part of the phase shift ϕ is directly proportional to the real part of the coherent scattering amplitude b_c for S-wave scattering to 10^{-4} accuracy even in a nucleus such as ^{3}He with a strong absorption cross section. It is clear that this approximation will break down in the presence of a scattering resonance, since in this case the phase shift is no longer small and the approximate expression for the scattering amplitude in terms of the phase shift is no longer valid.

III. EXPERIMENTAL PROCEDURE AND RESULTS

Our measurement of b_c for the n-^{3}He system was performed at the National Institute of Standards and Technology (NIST) Center for Neutron Research (NCNR) Interferometer and Optics Facility [18]. This facility consists of a perfect silicon crystal neutron interferometer, shown schematically in Fig. 1. A cold monochromatic neutron beam ($E = 11.1$ meV, $\lambda = 0.271$ nm, $\Delta\lambda/\lambda \leqslant 0.5\%$) enters the facility and is coherently divided via Bragg diffraction into two beams that travel along paths I and II. These beams are again diffracted and then coherently recombined. A detailed description of the facility, experimental arrangement, and procedures for the determination of neutron coherent scattering lengths can be found in Ref. [11].

The bound coherent scattering length, b_c, can be determined using neutron interferometric techniques. It is directly proportional to the neutron optical potential that gives rise to the phase shift between the two arms of the interferometer. This phase shift is given by

$$\phi = -\lambda N D_{eff} b_c, \tag{15}$$

where λ is the neutron wavelength, N is the atomic number density, and D_{eff} is the effective (geometric) thickness of the sample [19]. Corrections to this relation between the phase shift and the optical potential are small compared to presently achievable accuracies [19,20]. To measure b_c to 0.1% absolute accuracy, the neutron optical phase shift ϕ, the atom density, the sample thickness, and the neutron wavelength must each be measured to a precision of at least 0.04%.

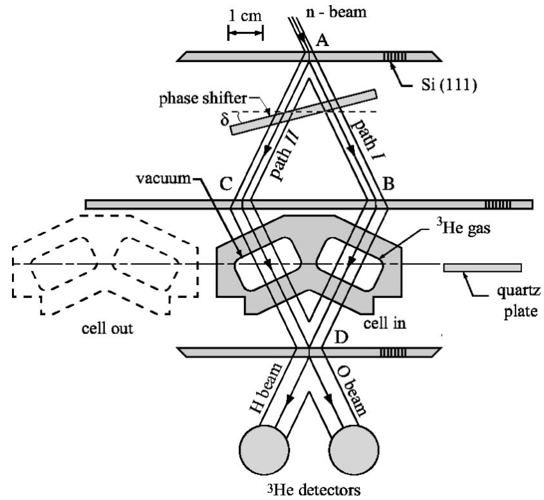

FIG. 1. A schematic view of the Si perfect crystal neutron interferometer. Parameters associated with the neutron optics are discussed in the text.

A secondary sampling method is used to measure the phase shift ϕ due to the gas sample. This is accomplished by positioning a rotatable quartz phase shifter across the two beams as shown in Fig. 1. The intensities of the beams that arrive at the two ^{3}He detectors are a function of the phase shifter angle δ and are given by

$$I_{\mathrm{O}}(\delta) = A_{\mathrm{O}} + B\cos[Cf(\delta) + \phi + \phi_{cell}],$$

$$I_{\mathrm{H}}(\delta) = A_{\mathrm{H}} + B\cos[Cf(\delta) + \phi + \phi_{cell} + \pi]. \tag{16}$$

The values of A_{O}, A_{H}, B, and C are extracted from fits to the data. The function $f(\delta)$ depends on the Bragg angle θ_B and is a measure of the neutron optical path length difference between the beams induced by the phase shifter and is given by

$$f(\delta) = \frac{\sin(\theta_B)\sin(\delta - \delta_0)}{\cos^2(\theta_B) - \sin^2(\delta - \delta_0)}. \tag{17}$$

The ^{3}He gas is housed in a cell specifically designed to minimize the phase shift ϕ_{cell} due to the aluminum walls of the cell (see Fig. 1). ^{3}He gas (99.999% chemically pure, 99.99% isotopically pure [21,22]) at a pressure of 3.380×10^5 Pa (3.34 atm) was introduced into path I, while keeping the chamber in path II evacuated. The phase shifts arising from the presence of the ^{3}He gas and cell (ϕ_{gas} and ϕ_{cell}) were determined by collecting $\approx 10^3$ interferogram pairs with the cell positioned both within the interferometer and removed from the beam paths. The phase difference between cell-in /cell-out sets of interferograms is extracted for each pair, with a typical set shown in Fig. 2. This procedure was repeated with both chambers evacuated to determine the phase shift arising from the difference in aluminum wall thickness between the two chambers of the target cell. The cell phase shift ϕ_{cell} was determined to be $\phi_{cell} = (-1.379 \pm 0.002)$rad.

[1]The derivation performed in Ref. [17] is in a solid and thus $b_c = a_c$.

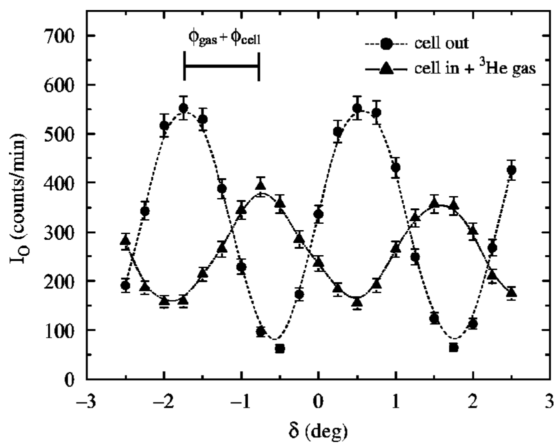

FIG. 2. A typical pair of interferograms with ^{3}He present in the cell. The oscillations arise from the change in path lengths created as the phase shifter is rotated (see Fig. 1). Data are shown for both the cell in and out of the interferometer.

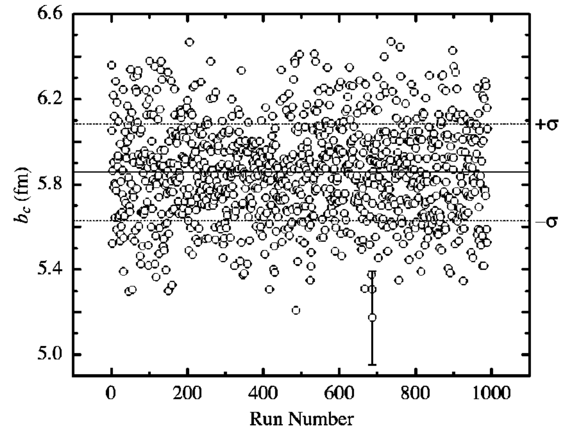

FIG. 3. Measurements of the coherent scattering length b_c plotted on a run-by-run basis. Each data point represents approximately 42 min of data. The solid line is the weighted average of the data, $b_c=(5.8572\pm0.0072)$fm. The estimated uncertainty for one of the data points is shown.

The atom density was determined using the ideal gas law with virial coefficient corrections up to the third pressure coefficient. Values for these coefficients are $B_P=4.797\times10^{-9}$ Pa^{-1} and $C_P=-1.129\times10^{-17}$ Pa^{-2},[2] and are obtained from Refs. [23,24]. Note that the correction for C_P has no effect on the final result. The absolute temperature was continuously monitored using two calibrated 100 Ω platinum thermometers that have an absolute accuracy of 0.023% at 300 K. The pressure was continuously monitored using a calibrated silicon pressure transducer capable of measuring the absolute pressure to better than 0.01%. The wavelength of neutrons traversing the interferometer was measured using a pyrolytic graphite (PG 002) crystal. This analyzer crystal, calibrated separately against a Si crystal, was placed in the H beam of the interferometer and rotated such that both the symmetric and antisymmetric Bragg reflections were determined. Using this technique, the mean wavelength was determined to be $\lambda=(0.271207\pm0.000005)$nm. In a separate test, the stability of the wavelength over time was shown to be 0.001%. More details on the measurement techniques and systematic uncertainties involved in the determination of the neutron wavelength, atom density, temperature, and cell thickness, which were identical to those used in our previous measurements of the *n-p* and *n-d* coherent scattering lengths, can be found in Ref. [11].

The cell's effective thickness depends on the true cell thickness D_0 and the horizontal and vertical tilt angles with respect to the neutron beam direction, $\Delta\epsilon$ and $\Delta\gamma$, respectively, according to

$$D_{eff}=\frac{D_0}{\cos\Delta\epsilon\cos\Delta\gamma}. \tag{18}$$

The thickness of the gas cell, D_0, was measured using the NIST Precision Engineering Division Coordinate Measuring Machine [25] and determined to be (1.0016 ± 0.0001) cm and is uniform at the 0.01% level. The thickness was corrected for thermal expansion and contraction due to temperature fluctuation for each individual run. The change in thickness of the cell due to the gas pressure is negligible. $\Delta\epsilon$ and $\Delta\gamma$ were measured independently and both were set such that their values are consistent with zero. The upper bounds for both $\Delta\epsilon$ and $\Delta\gamma$ are 2 mrad, which gives a negligible change in the thickness.

The value of the bound coherent scattering length was calculated for each data set on a run-by-run basis and is shown in Fig. 3. These values are combined using a weighted average to obtain $b_c=(5.8572\pm0.0072)$fm. A more detailed treatment of the statistical uncertainties associated with interferometric scattering length measurements is also given in Ref. [11]. Table I summarizes the parameters and relative uncertainties of all parameters used to extract b_c. The upper limit on the uncertainty arising from the manufacturer's stated impurities in the ^{3}He (including ^{4}He) is 4×10^{-5}, roughly two orders of magnitude smaller than the statistical uncertainty.

TABLE I. Parameters and relative uncertainties required to determine the scattering length. The values given for the temperature, pressure, and atom density represent the average values during data collection. Corrections for variations in these parameters are made on a run-by-run basis. The uncertainty in our coherent scattering length measurement is dominated by the statistical uncertainty in the phase shift difference ϕ.

Parameter	Value	Relative σ
ϕ	2.69 rad	6.6×10^{-4}
λ	0.271207 nm	2.0×10^{-5}
Temperature	23.237 °C	2.3×10^{-4}
Pressure	3.380×10^5 Pa	1.0×10^{-4}
N	8.250×10^{19} cm^{-3}	3.5×10^{-4}
D_0	1.0016 cm	1.0×10^{-4}

[2]The value for C_P was taken from ^{4}He data.

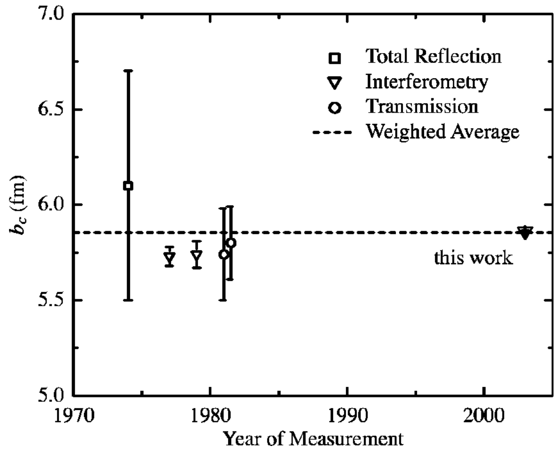

FIG. 4. Measured values of the ^{3}He neutron coherent scattering length including the present measurement [26–30]. The dashed line denotes the weighted average of all measurements, $b_c = (5.853 \pm 0.007)$fm.

IV. DISCUSSION AND FUTURE DIRECTIONS

Our value represents a factor of eight improvement in precision over any single previous measurement of b_c. Using the values published in Refs. [26–30], we obtain a value of $b_c = (5.74 \pm 0.04)$fm for the previous world average. Our value is larger than the previous world average by roughly three standard deviations (see Fig. 4), thus shifting the value for the present world average to $b_c = (5.853 \pm 0.007)$fm and improving the precision by a factor of six.

Measurements of the *n-p* [11], *n-d* [11,12], and *n*-^{3}He coherent scattering lengths have now been performed in an identical manner using the same apparatus (cell, neutron wavelength analyzer, and pressure and temperature monitors). The reported values are $b_{np} = (-3.7384 \pm 0.0020)$fm [11], $b_{nd} = (6.6649 \pm 0.0040)$fm [11,12], and $b_{n^3\mathrm{He}} = (5.8572 \pm 0.0072)$fm (this result). One can take the ratio of any two of these values to minimize any systematic effect that in principle could still remain. Although this ratio will possess additional statistical uncertainties, it will be independent of any unknown systematic uncertainty to first order. Using b_{np} as the reference, we obtain

$$b_{n^3\mathrm{He}}/b_{np} = (-1.5668 \pm 0.0021),$$

$$b_{nd}/b_{np} = (-1.7828 \pm 0.0014).$$

One can also extract considerably improved values for the real parts of the singlet and triplet neutron scattering lengths using the improved value of b_c. In a recent experiment, the value for the *n*-^{3}He bound incoherent scattering length, $b_i = (-2.365 \pm 0.020)$fm, was determined using nuclear pseudomagnetic precession in a polarized ^{3}He target placed in a neutron spin echo spectrometer [14]. This value represents an impressive improvement of a factor of 30 over previous measurements. Combining the new value of b_i with the new world average of b_c, one obtains considerably improved values for the singlet and triplet bound scattering lengths:

$$b_0 = (9.949 \pm 0.027)\mathrm{fm},$$

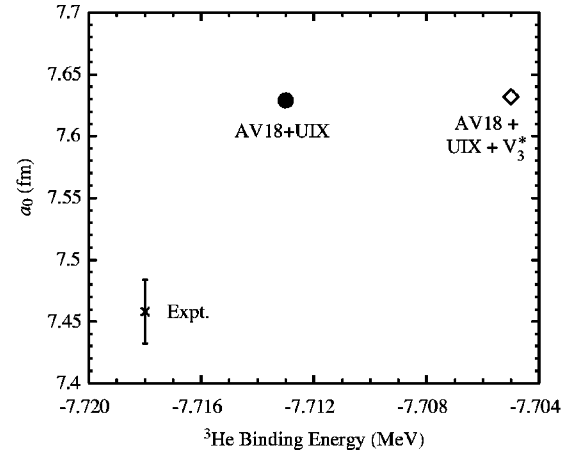

FIG. 5. Comparison of the experimental and theoretical determinations of the free-atom singlet scattering length a_0. The theoretical values were calculated using the AV18+UIX and AV18+UIX+V_3^* potential models [32]. Note that the experimental uncertainty on the ^{3}He binding energy is negligibly small $E_{bind} = -7.718109 \pm 0.000010$ MeV [36].

$$b_1 = (4.488 \pm 0.017)\mathrm{fm}.$$

Using the recommended values for the atomic ^{3}He mass and neutron mass [31] and Eq. (2), the free nuclear singlet and triplet scattering lengths are then

$$a_0 = (7.456 \pm 0.020)\mathrm{fm},$$

$$a_1 = (3.363 \pm 0.013)\mathrm{fm}.$$

We note that the uncertainty in these values is primarily due to the uncertainty in b_i.

The coherent scattering cross section

$$\sigma_c = 4\pi b_c^2 = (4.305 \pm 0.007)\mathrm{b}, \tag{19}$$

which, when added to the Zimmer *et al.* result for the incoherent scattering cross section, namely $\sigma_i = (1.532 \pm 0.012)$b [14], gives a new value for the scattering cross section,

$$\sigma_s = \sigma_c + \sigma_i = (5.837 \pm 0.014)\mathrm{b}. \tag{20}$$

Hofmann and Hale have recently published new calculations of the spin-dependent *n*-^{3}He scattering lengths using the resonating group method and a variety of modern *NN* and 3*N* potentials [32]. Comparisons of the experimental free nuclear singlet and triplet scattering lengths with theoretical calculations of these parameters were performed using the Argonne v_{18} (AV18) [33] *NN* potential with the Urbana IX (UIX) [8] and V_3^* [34,35] three-nucleon forces. The results of these calculations are shown in Figs. 5 and 6 alongside the experimental data.

The discrepancy between the calculated and the extremely well-known experimental value of the ^{3}He binding energy can be understood by noting that the number of J^π channels included in the calculation was limited in order to make it tractable. In addition, the three-body potentials used in the calculation were parameterized in terms of Gaussians, which seems to have induced a small shift in the calculated binding

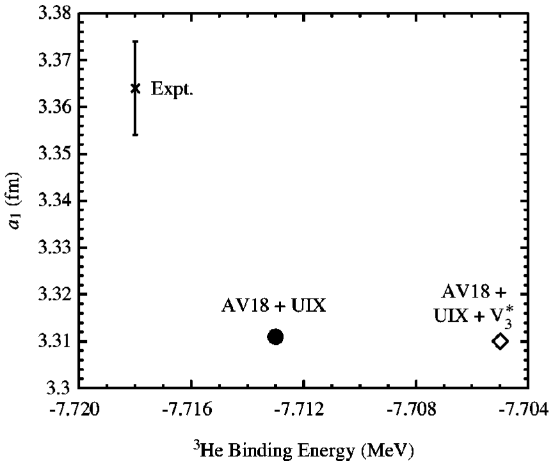

FIG. 6. Comparison of the experimental and theoretical determinations of the free-atom triplet scattering length a_1. The theoretical values were calculated using the AV18+UIX and AV18+UIX+V_3^* potential models [32].

energies. (For further details on the calculations, see Refs. [32,35].) It is clear however that the theoretical predictions from even these impressive, state-of-the-art calculations using resonating group techniques still lie outside the range of experimental uncertainties for the ^{3}He binding energy and the singlet and triplet scattering lengths.

One can also directly compare the experimental measurements of b_c and b_i with the combined values of the theoretically calculated singlet and triplet scattering lengths. This comparison is shown in Table II.

The theoretical calculations using the AV18+UIX and AV18+UIX+V_3^* potentials agree quite well with the measured value of b_c but fail to reproduce b_i. This disagreement is not entirely surprising. It has been shown that modern *NN* potentials, even with 3*N* forces adjusted to match the ^{3}He binding energy, disagree with the *n-d* coherent scattering length [11–13]. (We note that the AV18+UIX+V_3^* potential model has not been tested in this way.) Given this existing disagreement in the *n-d* system, one is not too surprised to see disagreement at comparable precision in the much more complicated *n*-^{3}He system. It would be interesting to compare exact four-body calculations of the *n*-^{3}He scattering lengths using modern potentials. As noted in the Introduction, the greatest potential utility of these measurements may come from their use in future EFT-based calculations of observables in the four-nucleon system.

It is also interesting to consider how the experimental determinations of the *n*-^{3}He scattering lengths can be further improved. Our measurement of the coherent scattering length is dominated by statistical uncertainties in the measurement of the phase shifts and consequently there is still room for improvement. In the case of the incoherent scattering length determination from pseudomagnetic precession performed by Zimmer *et al.* [14], the accuracy is unfortunately limited by the poor experimental knowledge of the relative contributions of singlet and triplet channels to the *n*-^{3}He absorption cross section. A better measurement of this ratio, currently known to ≈1% [37,38], could be immediately combined with the Zimmer *et al.* measurement to improve the accuracy of b_i by as much as a factor of three. In addition, a new measurement currently being planned at NIST to directly measure the spin-dependent *n*-^{3}He scattering lengths is independent of this ratio [39]. Dramatically reduced uncertainties for a_0 and a_1 in *n*-^{3}He are therefore possible.

TABLE II. Comparison of the calculated and experimental values of the coherent scattering length b_c and the incoherent scattering length b_i. The four potential model calculations are taken from Ref. [32] and formed by combining the individual singlet and triplet scattering lengths using Eq. (1) or (3). No single theory agrees with both b_c and b_i. The experimental values are taken from this work and Ref. [14].

Potential	b_c(fm)	b_i(fm)
AV18	6.050 ± 0.002	-2.509 ± 0.003
AV18+UIX	5.859 ± 0.001	-2.495 ± 0.001
AV18+UIX+V_3^*	5.859 ± 0.001	-2.497 ± 0.001
R matrix	5.757 ± 0.006	-2.377 ± 0.004
Experiment	5.857 ± 0.007	-2.365 ± 0.020

The fact that three precisely measured neutron scattering lengths in few-body systems are now all in disagreement with the best current theories is intriguing. These results may imply that high-precision low-energy neutron scattering lengths now possess more sensitivity than nuclear binding energies and energy levels to small effects such as nuclear three-body forces, charge symmetry breaking, and residual electromagnetic effects not yet fully included in current models. We also note that it would be possible to perform high precision coherent neutron scattering length measurements in other few-body systems. In particular, our techniques could be extended to perform high precision coherent scattering length measurements in *n*-^{3}H and *n*-^{4}He. Although the more interesting *n*-^{3}H measurement possesses experimental difficulties due to the radioactive nature of the target, *n*-^{4}He could easily be performed. There is also a separate proposal to perform a high precision measurement of b_i in the *n-d* system [40]. We encourage theorists in the field to consider including the calculation of neutron scattering lengths along with binding energies and energy levels in nuclear few body systems and make predictions that can be tested by new precision experiments.

ACKNOWLEDGMENTS

We would like to thank the NIST Center for Neutron Research for use of the neutron facilities during this experiment. This work was supported in part by the U.S. Department of Commerce and the National Science Foundation under Grant Nos. PHY-9603559 at the University of Missouri, PHY-9602872 at Indiana University, and PHY-0245679 at the University of North Carolina at Wilmington.

[1] J. L. Friar, B. F. Gibson, and G. L. Payne, Phys. Rev. C **28**, 983 (1983).
[2] S. Ishikawa, Phys. Rev. C **59**, R1247 (1999).
[3] H. Witała, D. Hüber, and W. Glöckle, Few-Body Syst. **14**, 171 (1993).
[4] W. Glöckle, H. Witała, D. Hüber, H. Kamada, and J. Golak, Phys. Rep. **274**, 107 (1996).
[5] A. Kievsky, M. Viviani, and S. Rosati, Phys. Rev. C **52**, R15 (1995).
[6] S. Rosati, M. Viviani, and A. Kievsky, Few-Body Syst., Suppl. **8**, 21 (1995).
[7] A. Kievsky, Few-Body Syst., Suppl. **9**, 405 (1995).
[8] B. S. Pudliner, V. R. Pandharipande, J. Carlson, S. C. Pieper, and R. B. Wiringa, Phys. Rev. C **56**, 1720 (1997).
[9] J. Carlson and R. Schiavilla, Few-Body Syst., Suppl. **7**, 349 (1994).
[10] A. Ioffe, D. L. Jacobson, M. Arif, M. Vrana, S. A. Werner, P. Fischer, G. L. Greene, and F. Mezei, Phys. Rev. A **58**, 1475 (1998).
[11] K. Schoen, D. L. Jacobson, M. Arif, P. R. Huffman, T. C. Black, W. M. Snow, S. K. Lamoreaux, H. Kaiser, and S. A. Werner, Phys. Rev. C **67**, 044005 (2003).
[12] T. C. Black, P. R. Huffman, D. L. Jacobson, W. M. Snow, K. Schoen, M. Arif, H. Kaiser, S. K. Lamoreaux, and S. A. Werner, Phys. Rev. Lett. **90**, 192502 (2003).
[13] H. Witała, A. Nogga, H. Kamada, W. Glöckle, J. Golak, and R. Skibiński, Phys. Rev. C **68**, 034002 (2003).
[14] O. Zimmer, G. Ehlers, B. Farago, H. Humblot, W. Ketter, and R. Scherm, EPJdirect **1**, 1 (2002).
[15] A. Abragam and M. Goldman, *Nuclear Magnetism: Order and Disorder* (Clarendon, Oxford, 1982).
[16] E. Epelbaum, H. Kamada, A. Nogga, H. Witała, W. Glöckle, and Ulf-G. Meissner, Phys. Rev. Lett. **86**, 4787 (2001).
[17] M. L. Goldberger and F. Seitz, Phys. Rev. **71**, 294 (1947).
[18] M. Arif, D. E. Brown, G. L. Greene, R. Clothier, and K. Littrell, Proc. SPIE **2264**, 21 (1994).
[19] H. Rauch and S. Werner, *Neutron Interferometry: Lessons in Experimental Quantum Mechanics* (Oxford University Press, New York, 2000).
[20] V. F. Sears, *Neutron Optics* (Oxford University Press, New York, 1989).
[21] Spectra Gases, 80 Industrial Drive, Alpha, NJ 08865.
[22] Certain trade names and company products are mentioned in the text or identified in illustrations in order to adequately specify the experimental procedure and equipment used. In no case does such identification imply recommendation of endorsement by the National Institute of Standards and Technology, nor does it imply that the products are necessarily the best available for the purpose.
[23] J. J. Hurly and M. R. Moldover, J. Res. Natl. Inst. Stand. Technol. **105**, 667 (2000).
[24] J. H. Dymond, *The Virial Coefficients of Pure Gases and Mixtures: A Critical Compilation* (Oxford University Press, New York, 1980).
[25] J. Stoup, NIST Test No. 821/265253-01.
[26] T. A. Kitchens, T. Oversluizen, and L. Passell, Phys. Rev. Lett. **32**, 791 (1974).
[27] H. Kaiser, H. Rauch, W. Bauspiess, and U. Bonse, Phys. Lett. **71B**, 321 (1977).
[28] H. Kaiser, H. Rauch, G. Badurek, W. Bauspiess, and U. Bonse, Z. Phys. A **291**, 231 (1979).
[29] V. P. Alfimenkov, S. B. Borzakov, Tkhuan Vo Van, A. M. Govorov, L. Lason', L. B. Pikel'ner, and E. I. Sharapov, Yad. Fiz. **33**, 891 (1981) [Sov. J. Nucl. Phys. **33**, 467 (1981)].
[30] M. Baumgartner, H. P. Gubler, M. Heller, G. R. Plattner, W. Roser, and I. Sick, Nucl. Phys. **A368**, 189 (1981).
[31] G. Audi and A. H. Wapstra, Nucl. Phys. **A595**, 409 (1995).
[32] H. M. Hofmann and G. M. Hale, Phys. Rev. C **68**, 021002(R) (2003).
[33] R. B. Wiringa, V. G. J. Stoks, and R. Schiavilla, Phys. Rev. C **51**, 38 (1995).
[34] L. Canton and W. Schadow, Phys. Rev. C **62**, 044005 (2000).
[35] B. Pfitzinger, H. M. Hofmann, and G. M. Hale, Phys. Rev. C **64**, 044003 (2001).
[36] A. H. Wapstra and G. Audi, Nucl. Phys. **A432**, 1 (1985).
[37] L. Passell and R. I. Schermer, Phys. Rev. **150**, 146 (1966).
[38] S. B. Borzakov, H. Malecki, L. B. Pikel'ner, M. Stempinski, and E. I. Sharapov, Yad. Fiz. **35**, 532 (1982) [Sov. J. Nucl. Phys. **35**, 307 (1982)].
[39] F. E. Wietfeldt (private communication).
[40] B. van den Brandt, H. W. Griesshammer, P. Hautle, J. Kohlbrecher, J. A. Konter, and O. Zimmer, to be published in Nucl. Instrum. Methods Phys. Res. A as part of the Proceedings of the 9th International Workshop on Polarized Solid Targets and Techniques in Bad Honnef, Germany, 2003, nucl-ex/0401029.